PROCEEDINGS OF SCIENCE

ref.bib

The optical properties of LHAASO atmospheric aerosol were observed by solar photometer

J J Xia,[a] F R Zhu,[a,*] J Liu[a] and H Liu[a]

[a] *School of Physical Science and Technology, Southwest Jiaotong University Chengdu, 611756, Sichuan Province, China*

E-mail: zhufr@swjtu.edu.cn

Large High Altitude Air Shower Observatory(LHAASO), located at 29.35°N, 100.13°E at an average altitude of 4410 meters on the Haizi Mountain in Daocheng County, Sichuan Province, China, is situated in the center of Hengduan Mountains (24°40′-34°00′N, 96°20′-104°30′ E). Hengduan Mountains are the transition zone of the Tibetan Plateau (TP), Sichuan Basin, and Yunnan-Guizhou Plateau, most of which belong to TP. The topography of Hengduan Mountains are complex, which are composed of plateau, alpine, canyon and basin and so on. They lie in the intersection of South Asia monsoon, East Asia monsoon and westlines, also controlled by westerly wind in winter and autumn period. The Wide Field-of-view Cherenkov Telescope Array (WFCTA), one of the three detector arrays at LHAASO, comprises 18 wide-field Cherenkov telescopes and is primarily utilized to accurately measure the 10^{13} to 10^{18} eV energy spectrum of the primary cosmic rays. The accuracy of observation of the WFCTA cosmic ray is influenced by variations in aerosols in the atmosphere. It is importance to understand well the optical characteristics of aerosols over the LHAASO. The solar photometer (CE-318T) was in normal operation at the LHAASO site from October 2020 to October 2022, and a total of 394 days and 23254 sets of valid observation data samples were obtained, excluding cloudy weather. Data analysis results after on-site field calibration showed that the annual average aerosol optical depth at 440 nm (AOD_{440nm}) was 0.05 ± 0.03, and the annual average Angstrom exponent at 440-870 nm ($AE_{440-870nm}$) was 1.17 ± 0.30. The monthly average maximum of AOD_{440nm} occurred in April (0.11 ± 0.05) and the minimum was in November (0.03 ± 0.01). The monthly average maximum of $AE_{440-870nm}$ was in June (1.36 ± 0.29) and the minimum was in December (0.91 ± 0.19). These results provide a basis for the calibration of photon number and reconstruction of extensive air shower observed by WFCTA.

38th International Cosmic Ray Conference (ICRC2023)
26 July - 3 August, 2023
Nagoya, Japan

*Speaker

1. Introduction

LHAASO is a dual-task facility designed for cosmic rays physics and gamma ray astronomy studies at TeV and PeV energies ([1]). It consists of three interconnected detectors, Water Cherenkov Detector Array (WCDA), Kilometer Square Array (KM2A), and Wide Field-of-view Cherenkov Telescope Array (WFCTA), located at 4410 m above sea level in the Sichuan province of China. WFCTA, consisting of 18 telescopes, has been designed to measure the primary cosmic rays in the energy range of 10^{13} -10^{17} eV and extend the energy scales of the direct measurements to the extreme highly energies, with a different layout in different observation modes and energy ranges [2].

WFCTA is mainly used to observe the Cherenkov or fluorescence light generated by charged particles produced by cosmic rays entering the atmosphere [3]. The number of photons can be used for making a calorimetric estimatation of the energy of the primary cosmic ray, however, their production and transmission are affected by the atmospheric conditions. The aerosol component is the most variable term contributing to the atmospheric transmission function. Thus, to reduce the systematic uncertainties on air shower reconstruction using the Cherenkov or fluorescence technique as much as possible, aerosols have to be continuously monitored. The 3 N2 laser systems and 2 YAG laser system have been developed to operate since Oct. 2020 at the LHAASO to monitor the atmosphere and calibrate the WFCTA in the clear nights [4][5][6][7]. A CIMEL sun photometer of CE318-T is operational on-site of LHAASO since Oct. 2020 as shown in Figure 1(a) [8].

Aerosol optical depth (AOD) is one of the key measurement indicators of aerosol optical properties, which represents the attenuation of light under the scattering and absorption of aerosol particles. AOD measurements are usually derived from ground measurements and satellite observations. The CE318-T has the advantages of high time resolution and low uncertainty (~0.01-0.02) in continuous measurement[9]. This device can provide daily measurement of aerosol and water vapor column content as data for atmospheric monitoring.

LHAASO (29.35°N, 100.13°E, 4410.0 m a.s.l.) is situated in the center of the Hengduan Mountains shown in the Figure1(b), the junction with the southeastern edge of the TP, the Yunnan-Guizhou Plateau and the Sichuan Basin as shown in the solid black rectangle of Figure 1(a). And has an average elevation of 4410 m above sea level [2]. The Hengduan Mountains are the easternmost and southernmost monsoonal temperate glacial region in Eurasia and are sensitive to climate change based on the research with glaciers and environments made by Chinese glaciologists, temperature and precipitation by meteorologist[10]. However, there are few studies on AOD variation from ground-based measurements, primarily owing to the lack of easily available data collection for the region. In 1983 and 1984 aerosol turbidity coefficient recorded in history was measured at 3 different elevation sites of Yunling Baimang Snow Mountain and the maximum turned in March and April. From Dec. 2009 Shangri-La atmosphere background station (28.01°N, 99.44°E, 3580.0 m a.s.l.) has been in business observation, but the variation of AOD with sun photometer has not be reported[11]. In 2017 ground measurements from the remote sensing network of AERONET were conducted at the Litang station (30.00°N, 100.16°E, 3950.5 m a.s.l.), approximately 70 km away from LHAASO in Google Map shown in Figure1(b). Litang has a similar topography with LHAASO, and a CE-318 sun photometer was used, which indicated a maximum in summer. However, Litang's observation only covers one year of data with invalid month of April and June

[12]. In addation, the CE-318 at Litang was installed in an urban station, while LHAASO is situated in the field, which is less affected by human activities and provides a better reflection of the characteristics in atmosphere background aerosols in Hengduan Mountains [13].

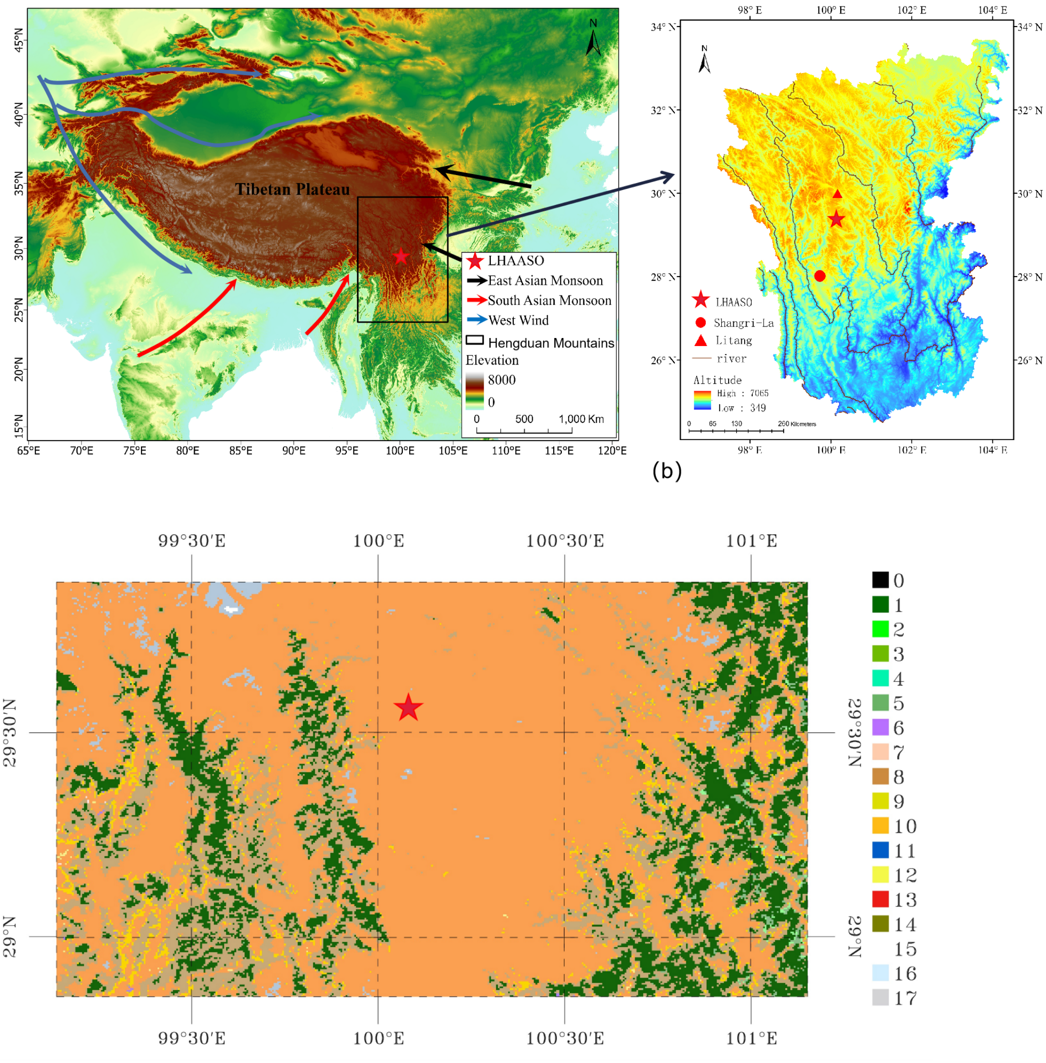

Figure 1: (a) Large-scale atmospheric circulation and topographic maps (in meters) of TP and the location of the LHAASO site in this study. (b) Topographic map of Hengduan Mountains and the location of LHAASO site for this study. (c) Geomorphological map of LHAASO (0 for water, 1 for evergreen needle leaf, 2 for evergreen broad leaf, 3 for deciduous needle leaf, 4 for deciduous board leaf, 5 for mixed forests, 6 for closed shrub lands, 7 for open shrub lands, 8 for woody savannas, 9 for savannas, 10 for grasslands, 11 for permanent wet lands, 12 for croplands, 13 for urban and built up, 14 for crop nat veg mosaic, 15 for snow and ice, 16 for barren or sparse, 17 for unclassified)

2. Methodology

2.1 Observation site

LHAASO (29.35°N, 100.13°E, 4410.0 m a.s.l.) is situated in the Haizi Mountain Nature Reserve in the eastern edge of the TP, the center of Hengduan Mountains, China. There exist both expansive and restrictive definitions of the boundary of the Hengduan Mountains. While Liu referred to the former, we adopt the latter for the purpose of this discussion[14]. As shown in the FIg:0(a). Hengduan Mountains (24°40′-34°00′N, 96°20′-104°30′ E) lie in the southeastern part of Tibetan Plateau, with an area of 500,000 km^2[10]. The region consists of a series of mountain ranges andrivers running from north to south, and the topography declines from northwest to southeast. All the rivers drains into the Pacific Ocean except for the Nujiang River, which is a part of the Indian Ocean water-system[15]. Characterized by north-south rivers and mountains aligned from west to east, it is an obstruction to the eastern Asia monsoon and a thoroughfare to the southern Asia monsoon. Hengduan Mountains belongs to a typical monsoonal climate region, not only controlled by the South Asia monsoon but also the East Asia monsoon, also influenced by the westerlies [16][17]. Correspondingly, moisture transfer can be also characterized by the obvious seasonal change. In summer, moisture mostly originates from the Bay of Bengal and the South China Sea, and is mainly obtained from the western Pacific Ocean in autumn. The winter monsoon period is from December to April and May to October is the summer monsoon period.

As is shown in Figure1(c), LHAASO is characterized by grasslands covered with sandy soil and small rocks, and a river that is 1-3 meters wide flows from the southwest to the northeast. Moreover, LHAASO is relatively isolated from industrial areas and cities with a very limited local population. It is located in the center of the Haizi Mountain Nature Reserve, spanning from 29.06°N to 30.06°N and from 99.33°E to 100.31°E. Seated in the south of the Haizi Mountain, the famous Aden Snow Mountains' average altitude is above 6000 m. The distribution of typical mountains makes the observation site influenced by local mountain.

2.2 Data quality monitoring

CE-318T has a higher gain and stronger signal than CE-318 [8]. To ensure the representativeness of the observations, we followed the uniform aeronautical standard[18]and considered no less than three observation days valid, provided that the instrument was functioning normally and the Sun was not entirely obscured by clouds. To minimize the impact of cloud cover, we employed an infrared cloud-sky instrument, which scans the entire sky in three dimensions to generate a brightness-temperature distribution map of infrared radiation and obtain fine-grained measurements of cloud shape and amount[19]. The ambient temperature measured at the LHAASO weather station, subtracting a fixed temperature of 55 degrees, to correct for the effect of cloudless weather on the infrared temperature of the cloud instrument at an elevation angle of 65 degrees. The CE-318T has been in operation since October 26, 2020, and is calibrated for automatic observations with 15-minute intervals. Till October 25, 2022, a total of 23254 data sets of observations have been collected after selection. As is shown in the Figure2(b), this resulted in a cumulative count of 389 effective observation days. The difference in data volume from month to month is mainly due to the weather. The data in June, July and August were relatively low mainly because it was in the rainy season and there were more cloudy days.

(a) 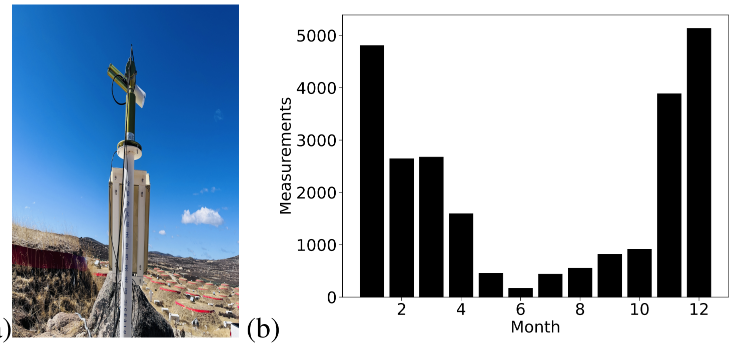 (b)

Figure 2: (a) CE-318T in the field observations. (b) The number of measurements VS month, some months may have less data because of the cloudy weather

3. Results and discussion

3.1 Meteorological conditions

Meteorological elements have a certain influence on AOD. However, under different environment and condition, their contributions are different to the variation of AOD. Temperature can often promote the increasing of AOD, while the influence of relative humidity (RH) and wind speed are more complex. Topography is also important factor to the AOD.

The on-site measurement of the temperature, relative humidity and wind speed are shown in Figure3, the average temperature for the 2020-2022 measurement period was 1.2 °C, with the maximum 9.1 °C and minimum -9.2 °C of monthly mean value. The higher temperature appeared from May to October. Similarly, the higher relative relative humidity was in May through October with more than 70%. The average annual relative humidity is 60%. The average annual wind speed was 2.0 m/s and the monthly mean wind speed occurred lower in the summer and heavier in the other 3 seasons. In all, during the winter observation period, conditions were very dry and cold. The meteorological conditions in the near-surface environment undergo seasonal shifts between the summer and winter seasons, characterized by fluctuations in air temperature from high to low, variations in relative humidity from wet to dry, and alterations in near-surface wind intensity from weak to strong.

3.2 Monthly variations of the ground-based AOD and AE

The Angstrom exponent (AE) is an important optical property of aerosol particles. It reflects the wavelength dependence of AOD and the spectral distribution of aerosol particles in the vertical gas column, providing information about the size characteristics of the particles[20].

According to the calibration results, the change of AOD at LHAASO was calculated. To better understand the time-dependent characteristics of AOD variation, we analyzed data from the entire year of 2020-2022. The average AOD at 440 nm (AOD_{440nm}) for the year was found to be 0.05 ± 0.03. The AE were measured for the 440 nm-870 nm wavelength range. During the measurement period of 2020-2022, the annual average $AE_{440-870nm}$ was 1.17 ± 0.30, as shown in Figure4. The monthly variation of $AE_{440-870nm}$ indicated a maximum in June (1.36 ± 0.29) and a minimum in

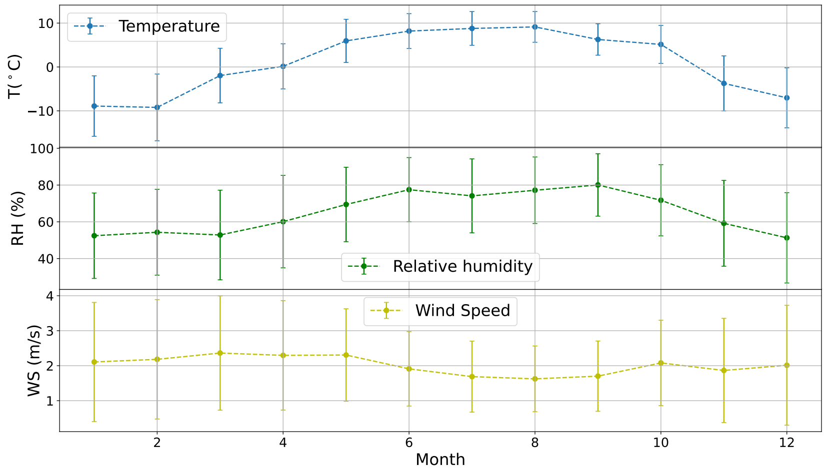

Figure 3: Time series of temperature, relative humidity, and wind speed during observation period

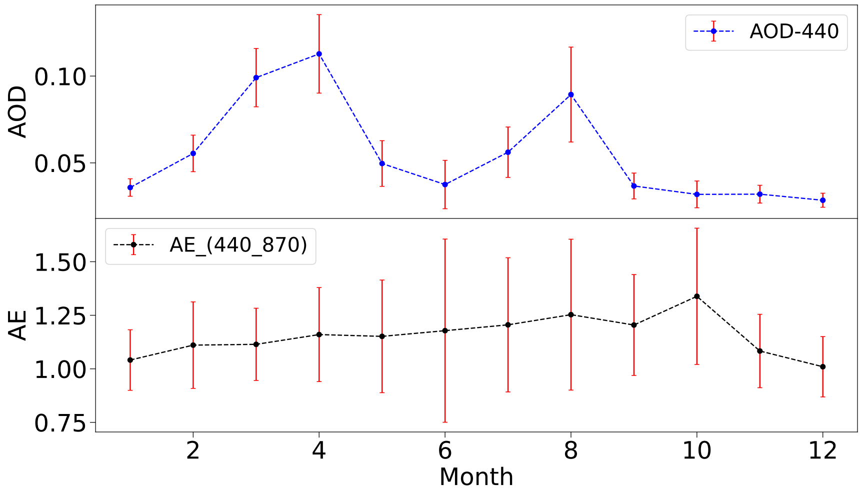

Figure 4: Monthly mean AOD_{440nm} with standard error (black dots) and monthly mean $AE_{440-870nm}$(blue dots) with standard error from ground-based measurements at the LHAASO site during the observation period.

December (0.91 ± 0.19). Daily mean aerosol in 2020-2022 are shown in Figure4. The monthly mean AOD_{440nm} reached a maximum in April (0.11 ± 0.05) and a minimum in November (0.03 ± 0.01). The aerosol content at LHAASO exhibited a bimodal structure, with higher values in March, April, and August and lower values in the remaining months. Overall, the aerosol content at LHAASO was relatively low and the atmosphere is relatively clean.

Located in the wilderness at the southeastern edge of the TP, LHAASO experiences less anthropogenic activity. The overall AOD results showed a high value in spring and summer and a lower value in autumn and winter. The changes in aerosol optical properties in this area are closely related to local meteorological conditions and the overall transport of aerosols on the TP.

4. Summary

TP plays a crucial role in the atmospheric circulation, energy budget, and hydrological cycles of the Asian region, and even globally, through both dynamical and thermal processes. Therefore, investigating the impact of aerosol on the climate and environment over the TP is of great significance. To achieve this, changes in AOD and AE over time were analyzed using solar photometer data from October 2020 to October 2022.

Data analysis results showed that the annual average AOD_{440nm} was 0.05 ± 0.03, and the annual average $AE_{440-870nm}$ was 1.17 ± 0.30. The monthly average maximum value of AOD_{440nm} occurs in April (0.11 ± 0.05) and the minimum value was in November (0.03 ± 0.01). The monthly average maximum value of $AE_{440-870nm}$ was in June (1.36 ± 0.29) and the minimum value was in December (0.91 ± 0.19). [sorting=none]

References

[1] Huihai He and LHAASO collaboration. Design of the LHAASO detectors. *Radiation Detection Technology and Methods*, 2:1–8, 2018.

[2] Cao Zhen, Chen Ming-Jun, Chen Song-Zhan, Hu Hong-Bo, Liu Cheng, Liu Ye, Ma Ling-Ling, Ma Xin-Hua, Sheng Xiang-Dong, Wu Han-Rong, et al. Introduction to large high altitude air shower observatory (LHAASO). *Chinese Astronomy and Astrophysics*, 43(4):457–478, 2019.

[3] X Bai, BY Bi, XJ Bi, Z Cao, SZ Chen, Y Chen, A Chiavassa, XH Cui, ZG Dai, D della Volpe, et al. The Large High Altitude Air Shower Observatory (LHAASO) Science White Paper–2021 Edition. *arXiv e-prints*, pages arXiv–1905, 2019.

[4] Fengrong Zhu, Yong Zhang, Ning Xie, Huan Yu Jia, and Xiu Mei Li. Study on the calibration optimization of the laser lidar for WFCTA of LHAASO. *35th International Cosmic Ray Conference*, 366(2):1, 2017.

[5] N Xie, H Liu, Y Hu, W Long, H Jia, F Zhu, and Q Chen. The performance of the laser systems in the calibration system of lhaaso-wfcta. In *36th International Cosmic Ray Conference (ICRC2019)*, volume 36, page 498, 2019.

[6] Long Chen, Xin Li, Lisi Ge, Hu Liu, Qinning Sun, Yang Wang, Junji Xia, Fengrong Zhu, Yong Zhang, et al. Application of the nitrogen laser calibration system in lhaaso-wfcta. 2021.

[7] QN Sun, LS Geng, X Li, L Chen, H Liu, Y Wang, FR Zhu, Y Zhang, Zhen Cao, F Aharonian, et al. The yag lidar system applied in lhaaso. 2021.

[8] África Barreto, Emilio Cuevas, María-José Granados-Muñoz, Lucas Alados-Arboledas, Pedro M Romero, Julian Gröbner, Natalia Kouremeti, Antonio F Almansa, Tom Stone, Carlos Toledano, et al. The new sun-sky-lunar Cimel CE318-T multiband photometer–a comprehensive performance evaluation. *Atmospheric Measurement Techniques*, 9(2):631–654, 2016.

[9] Manu Mehta, Ritu Singh, Ankit Singh, Narendra Singh, et al. Recent global aerosol optical depth variations and trends—A comparative study using MODIS and MISR level 3 datasets. *Remote sensing of environment*, 181:137–150, 2016.

[10] Zongxing Li, Yuanqing He, Chunfen Wang, Xufeng Wang, Huijuan Xin, Wei Zhang, and Weihong Cao. Spatial and temporal trends of temperature and precipitation during 1960–2008 at the hengduan mountains, china. *Quaternary International*, 236(1-2):127–142, 2011.

[11] Zou LI, Xiang-dong YANG, Zhi-jun BO, Tao MA, and Wei-li LIN. An introduction to environmental characteristics in background atmosphere station over shangri-la. *Journal of Yunnan University*, 33(s1)(8):237–242, 2011.

[12] Yingchang You, Tianliang Zhao, Yong Xie, Yu Zheng, Jun Zhu, Junrong Xia, Le Cao, Chenggang Wang, Huizheng Che, Yao Liao, et al. Variation of the aerosol optical properties and validation of MODIS AOD products over the eastern edge of the Tibetan Plateau based on ground-based remote sensing in 2017. *Atmospheric Environment*, 223:117257, 2020.

[13] Bin Liu, Zhiyuan Cong, Yuesi Wang, Jinyuan Xin, Xin Wan, Yuepeng Pan, Zirui Liu, Yonghong Wang, Guoshuai Zhang, Zhongyan Wang, et al. Background aerosol over the Himalayas and Tibetan Plateau: observed characteristics of aerosol mass loading. *Atmospheric Chemistry and Physics*, 17(1):449–463, 2017.

[14] Yu Liu and Liang Zhao. The preliminary analysis of sunshine durations with meteorological data for the chinese giant solar telescope site survey. *Monthly Notices of the Royal Astronomical Society*, 434(2):1674–1680, 2013.

[15] Weichen Tao, Gang Huang, Danhong Dong, Pengfei Wang, Ting Yu, and Hainan Gong. Dominant modes of interannual variability in precipitation over the hengduan mountains during rainy seasons. *International Journal of Climatology*, 41(4):2795–2809, 2021.

[16] Zongxing Li, Yuanqing He, Chunfen Wang, Xufeng Wang Wang, Huijuan Xin, Wei Zhang, and Weihong Cao. Spatial and temporal trends of temperature and precipitation during 1960-2008 at the Hengduan Mountains, China. *Quaternary International*, 236(2):127–142, 2011.

[17] WW Fan, ZY Hu, XY Xun, et al. Review of qinghai-xizang plateau monsoon's evolution and climatic effects. *Plateau Meteorology*, 40(6):1294–1303, 2021.

[18] D Tanré, YJ Kaufman, BN e al Holben, B Chatenet, A Karnieli, F Lavenu, L Blarel, O Dubovik, LA Remer, and A Smirnov. Climatology of dust aerosol size distribution and optical properties derived from remotely sensed data in the solar spectrum. *Journal of Geophysical Research: Atmospheres*, 106(D16):18205–18217, 2001.

[19] Stephen Smith and Ralf Toumi. Measuring cloud cover and brightness temperature with a ground-based thermal infrared camera. *Journal of applied meteorology and climatology*, 47(2):683–693, 2008.

[20] Xia Xiangao, Chen Hongbin, and Wang Pucai. Aerosol properties in a Chinese semiarid region. *Atmospheric Environment*, 38(27):4571–4581, 2004.